Mon. Not. R. Astron. Soc. **315**, 89–97 (2000)

The structure of black hole magnetospheres – I. Schwarzschild black holes

Pranab Ghosh[1,2★†]
[1]*NASA Goddard Space Flight Center, Greenbelt, MD 20771, USA*
[2]*Tata Institute of Fundamental Research, Bombay 400 005, India*

Accepted 2000 January 6. Received 2000 January 6; in original form 1997 April 11

ABSTRACT

We introduce a multipolar scheme for describing the structure of stationary, axisymmetric, force-free black hole magnetospheres in the '3 + 1' formalism. We focus here on Schwarzschild space–time, giving a complete classification of the separable solutions of the stream equation. We show a transparent term-by-term analogy of our solutions with the familiar multipoles of flat-space electrodynamics. We discuss electrodynamic processes around disc-fed black holes in which our solutions find natural applications: (i) 'interior' solutions in studies of the Blandford–Znajek process of extracting the rotational energy of holes, and of the formation of relativistic jets in active galactic nuclei and 'microquasars'; (ii) 'exterior' solutions in studies of accretion disc dynamos, disc-driven winds and jets. On the strength of existing numerical studies, we argue that the poloidal field structures found here are also expected to hold with good accuracy for rotating black holes, except for the cases of the maximum possible rotation rates. We show that the closed-loop exterior solutions found here are not in contradiction with the Macdonald–Thorne theorem, as these solutions, which diverge logarithmically on the horizon of the hole $\mathcal{H}$, only apply to those regions that exclude $\mathcal{H}$.

Key words: accretion, accretion discs – black hole physics – galaxies: active – galaxies: jets – galaxies: nuclei.

1 INTRODUCTION

The impetus for the study of black hole magnetospheres arises from our desire to understand the central powerhouse in active galactic nuclei (AGN) and double radio sources. In a seminal paper, Blandford & Znajek (1977, hereafter BZ) proposed that magnetic fields threading the horizon $\mathcal{H}$ of a Kerr black hole can tap the rotational energy of the hole, transporting the energy in twin beams to power luminous double radio lobes. The structure of force-free magnetospheres surrounding Kerr black holes was discussed by BZ in a formal four-dimensional language, giving two specific examples of simple field structure: (i) a split monopole and (ii) a non-separable paraboloid (see Section 2).

In a pioneering effort to bridge the gap between the language of black hole electrodynamics and that of flat-space electrodynamics, with which astrophysicists are normally familiar, Thorne & Macdonald (1982, hereafter TM) and Macdonald & Thorne (1982, hereafter MT) introduced the '3 + 1' formalism, wherein the space–time was split up into three space directions and one, uniquely chosen, 'universal' time direction [see Section 2 for a brief description; a lucid exposition of the formalism is given in Thorne, Price & Macdonald (1986), hereafter TPM]. Expressed in this way, equations of black hole electrodynamics become remarkably similar to the equations of pulsar electrodynamics, and one can justifiably expect to carry the accomplishment, expertise and intuition of pulsar electrodynamics over to black hole electrodynamics.

It is surprising, therefore, that a formalism for describing the general field structure of black hole magnetospheres has not been constructed so far, although the methods of the '3 + 1' formalism are ideally suited for this. Indeed, it seems that only four specific, simple field structures in Schwarzschild space–time have ever been reported in the literature, and these appear to have been found ad hoc. Two of these are separable solutions of the stream equation (see Section 2): the monopole [and the related trivial generalization, the 'split monopole' (BZ; Macdonald 1984, hereafter M84)] and the uniform field (Wald 1974; Hanni & Ruffini 1976; M84). The others are non-separable solutions: (i) asymptotically paraboloidal field lines (BZ), and (ii) asymptotically vertical field lines with specified slopes on the equatorial plane (Ghosh & Abramowicz 1997, hereafter GA). Apparently, the curved-space–time analogue of our all-too familiar and highly

★ E-mail: pranab@tifr.res.in
† Senior NAS/NRC Fellow.

useful multipole description of electric and magnetic fields in flat-space electrodynamics has remained unnoticed so far.

This paper introduces the first steps towards evolving a general scheme for describing black hole magnetospheres in terms of their basic constituents, the multipolar 'interior' and 'exterior' solutions in the appropriate space–time. We focus in this work on the field structure of stationary, axisymmetric, force-free magnetospheres around Schwarzschild black holes. We give a complete characterization of separable solutions for the case in which the poloidal and toroidal fields are decoupled. We show that the angular parts of the stream functions which describe the magnetic field (see Section 2) are described by Gegenbauer polynomials. The radial parts of the stream functions divide themselves into two classes, interior and exterior solutions, in analogy with the nomenclature of flat-space electrodynamics. The former class is described by Jacobi polynomials, and the latter by Jacobi functions of the second kind. We demonstrate a clear analogy between the basic constituents of the Schwarzschild solutions and those of flat-space electrodynamics, identifying Schwarzschild monopoles, dipoles, quadrupoles and so on. We show that the existence of exterior solutions with closed field loops is not in conflict with the theorem proved by MT on the impossibility of closed field loops threading the horizon $\mathcal{H}$, because these solutions (which diverge logarithmically on $\mathcal{H}$) are only applicable to regions that exclude $\mathcal{H}$, entirely in analogy with the behaviour of exterior solutions of flat-space electrodynamics with respect to the origin. Indeed, our inability to find any solutions that have closed loops and remain finite on $\mathcal{H}$ is a confirmation of the MT theorem.

The studies of astrophysical processes involving black hole electrodynamics that benefit particularly from this approach include the following:

(i) BZ-process studies with 'realistic' field configurations suggested by recent numerical simulations (GA and references therein; particularly see Brandenburg et al. 1995; Balbus & Hawley 1998);

(ii) studies of magnetic coupling of our exterior solutions to accretion discs in relation to dynamo action, jets and hydromagnetic winds (Khanna & Camenzind 1992,1996; Königl & Kartje 1994; Blandford 1998);

(iii) studies of our interior solutions in relation to magnetohydrodynamic (MHD) models of jet formation and collimation in AGN and 'microquasars' (Camenzind 1995; Fendt 1997, hereafter F97; Koide, Shibata & Kudoh 1998, 1999, hereafter K98, K99; Eikenberry et al. 1998).

Distinct field geometries relevant for these different processes usually emerge naturally as low-order (see Section 5.4) examples of different classes of solutions identified in this work: we indicate these briefly, deferring detailed astrophysical applications to later works. Indeed, a main virtue of our multipolar approach to black hole electrodynamics is that a specific model field configuration is immediately identifiable as the natural choice for a given astrophysical problem, from symmetry considerations alone, without detailed computations.

Calculations for rotating black holes will be presented in a later work. We note here that, in a numerical study utilizing relaxation methods, M84 spun up Schwarzschild solutions corresponding to the first three of the four simple cases listed above, and showed that the effect of rotation on the *poloidal* field structure was very small in all cases: barely perceptible for $0 \leqslant a/M \leqslant 0.75$, where a/M is the angular momentum of the hole per unit mass. If this result is generally true, it is of basic importance as it would imply that, as far as the poloidal field structure is concerned, the rotation of the hole is not just a non-essential complication, but also an insignificant one (except at the fastest possible rotation rates). For astrophysical applications, the poloidal structures classified in this paper thus appear to be adequate in all cases that do not involve black holes rotating near the limiting rate. Recent numerical simulations of jet formation by Koide and collaborators (K98; K99; Koide et al. 1999, hereafter KMSK), using their general relativistic MHD code, support this conclusion: we return to this point in Section 5.4. In a recent numerical study of the stream equation, utilizing finite-element techniques, F97 computed field structures (also see Section 5.4) in Kerr space–time which join on smoothly to the asymptotic jet solutions given by Appl & Camenzind (1993). Finally, it must be clear on general grounds that the *toroidal* field strength is expected to depend significantly on the rotation rate of the hole. We discuss these points again in Section 5.4, and suggest that the effects of the hole rotation on magnetospheric structure may be of secondary importance in studies of the BZ process and related issues, while they may be crucial in understanding collimation and stability of jets in AGN and microquasars.

2 BLACK HOLE ELECTRODYNAMICS

2.1 The '3 + 1' formulation

Only the essentials of the '3 + 1' formulation of curved-space–time electrodynamics are presented here, as detailed expositions may be found in TM, MT and TPM. The four-dimensional formulation of black hole electrodynamics can be re-expressed in terms of the familiar electric, magnetic and current three-vectors, and the charge-density scalar of flat-space electrodynamics through the use of the following prescription. For each space–time event, one chooses a fiducial reference frame by performing a '3 + 1' division of space–time into three space directions and one, uniquely chosen, 'universal' time direction. One then decomposes the electromagnetic field tensor into the electric and magnetic field vectors in the usual manner, and the four-current density is also decomposed into the current three-vector and the charge density. Maxwell's equations (the continuity equation for charge and current density and the momentum equation) are then rewritten in terms of these variables.

In stationary black hole electrodynamics, the natural choice for the fiducial frame is that of a so-called zero angular momentum observer (ZAMO: see Bardeen, Press & Teukolsky 1973), who is at rest in the stationary gravitational field of the hole. For rotating holes, this further implies that the observer's angular velocity must be such that the observer's world lines appear orthogonal to a family of three-dimensional hypersurfaces of constant (Boyer–Lindquist) time (TPM). By mentally collapsing the entire collection of these constant-time hypersurfaces into a single three-dimensional space, which we can regard as an 'absolute space', we can envisage electrodynamics (and other physics) as occurring in this absolute three-space. Consequently, the universal time becomes a parameter that describes the evolution of matter and fields in this absolute space. This is the absolute-space/universal-time depiction of the 3 + 1 formalism, of which the analogy with Galilean relativity facilitates extension of astrophysical intuition into black hole electrodynamics (TM).

2.2 The stream equation

In the above framework the structure of a stationary, axisymmetric,

force-free black hole magnetosphere is specified by ψ, a scalar function of position called the *stream function*, and by two functions of ψ, namely the current potential I, and the angular velocity Ω_F of the magnetic field lines (M84). The poloidal and toroidal components of the magnetic field are given by

$$\boldsymbol{B}_p = \frac{\nabla\psi \times \hat{\boldsymbol{\phi}}}{2\pi\varpi} \tag{1}$$

and

$$\boldsymbol{B}_T = -\frac{2I}{\aleph\varpi}\hat{\boldsymbol{\phi}}, \tag{2}$$

respectively, with analogous expressions for the electric fields; the toroidal electric field is zero in an axisymmetric system. Here, ∇ is the gradient operator of the absolute three-space referred to above, i.e. it is the 'space–space' part of the four-dimensional metric of the space–time that we began with (M84). Furthermore, $\aleph$ is the so-called lapse function or gravitational redshift factor, i.e. the rate of lapse of the ZAMO's proper time relative to that of the universal time referred to above: it is the 'time–time' part of the four-dimensional metric. Finally, $\varpi = r\sin\theta$ is the cylindrical radius, and $\hat{\boldsymbol{\phi}}$ is a unit vector in the azimuthal direction.

The name 'stream function' was (apparently) coined by Newtonian analogy, because the poloidal magnetic field points everywhere along streamlines of ψ (i.e. poloidal lines of constant ψ): thus, poloidal field lines are contours of *constant* ψ (see equation 1). Applications of this description to magnetic fields are well-known in flat-space electrodynamics: see e.g. Michel's (1973, hereafter M73) work on pulsar electrodynamics, in which ψ was called a field-line label. Further analogies with flat-space electrodynamics may be made: ψ is proportional to the toroidal component of the vector potential (which, in turn, is related to the magnetic flux), and $I(r_0,\ \theta_0)$ is the total current through the azimuthal loop ($r = r_0,\ \theta = \theta_0$). The stream function satisfies a second-order elliptic differential equation which is variously called the stream equation (MT), the Grad–Shafranov or the trans-field equation (Beskin 1997; hereafter B97). The equation is

$$\nabla\cdot\left\{\frac{\aleph}{\varpi^2}\left[1-\frac{(\Omega_F-\omega)^2\varpi^2}{\aleph^2}\right]\nabla\psi\right\} + \frac{\Omega_F-\omega}{\aleph}\frac{\mathrm{d}\Omega_F}{\mathrm{d}\psi}(\nabla\psi)^2 + \frac{16\pi^2}{\aleph\varpi^2}I\frac{\mathrm{d}I}{\mathrm{d}\psi} = 0, \tag{3}$$

where ω is the angular velocity of the ZAMO rest frame relative to absolute space, i.e. the 'time–space' part of the four-dimensional metric referred to above.

For Schwarzschild black holes, $\Omega_F = \omega = 0$, so that the stream equation simplifies considerably. The lapse function is given in this case by

$$\aleph = \sqrt{1-\frac{2M}{r}}, \tag{4}$$

where M is the mass of the hole (we shall use the natural units, $G = c = 1$, throughout this paper). In this work, we study the black hole magnetospheres in which the current potential $I(\psi)$ is of such form that the last term on the left-hand side of equation (3) vanishes, so that the poloidal and toroidal fields are in some sense decoupled [for a different choice of $I(\psi)$, useful for modelling cylindrically collimated jets, see Appl & Camenzind (1993) and F97]. Two types of (astrophysically) important situations in which this condition holds have been described in the literature. The first type occurs when the black hole is immersed in a vacuum: all analytical Schwarzschild solutions reported by Wald (1974), Hanni & Ruffini (1976), BZ and M84 fall into this category. The second type corresponds to the situation described by GA, in which $I = I_0 =$ constant, so that $B_T \propto \aleph^{-1}\varpi^{-1}$ (see equation 2). In this case, the toroidal field scales asymptotically as $B_\phi \sim \varpi^{-1}$ far from $\mathcal{H}$ and diverges, of course, as $\aleph^{-1}$ (MT) when $\mathcal{H}$ is approached. This asymptotic behaviour is reminiscent of some of the Newtonian model solutions presented by Blandford (1976, hereafter B76), and is relevant to electrodynamics of accretion-disc-fed black holes, as emphasized by GA. In fact, these two types of situation are, to our knowledge, the only ones in which analytical Schwarzschild solutions of field structures around black holes have been reported so far. In these circumstances, the stream equation reduces to the linear differential equation

$$\nabla\cdot\left(\frac{\aleph}{\varpi^2}\nabla\psi\right) = 0. \tag{5}$$

2.3 Separable solutions

With the aid of equation (4) and the explicit form of ∇ for the Schwarzschild metric, equation (5) becomes

$$r^2\frac{\partial}{\partial r}\left[\left(1-\frac{2M}{r}\right)\frac{\partial\psi}{\partial r}\right] + \sin\theta\frac{\partial}{\partial\theta}\left(\frac{1}{\sin\theta}\frac{\partial\psi}{\partial\theta}\right) = 0. \tag{6}$$

In this work, we are principally concerned with *separable* solutions of equation (6), which offer a rich variety of multipolar structures. Only two non-separable solutions of equation (6) have been reported in the literature (BZ, M84, GA): we refer to these at appropriate places.

Separable solutions of equation (6) are of the form

$$\psi(r,\theta) = R(r)\Theta(\theta), \tag{7}$$

where the radial part R and the angular part Θ satisfy equations obtained by combining equations (6) and (7):

$$\frac{\mathrm{d}}{\mathrm{d}\theta}\left(\frac{1}{\sin\theta}\frac{\mathrm{d}\Theta}{\mathrm{d}\theta}\right) = -A\frac{\Theta}{\sin\theta} \tag{8}$$

and

$$\frac{\mathrm{d}}{\mathrm{d}r}\left[\left(1-\frac{2M}{r}\right)\frac{\mathrm{d}R}{\mathrm{d}r}\right] = A\frac{R}{r^2}, \tag{9}$$

where A is the separation constant.

3 SOLUTIONS OF THE STREAM EQUATION

3.1 Lowest-order solutions

Solutions of equations (8) and (9) in the special case of $A = 0$ constitute the lowest-order separable solutions of the stream equation. In the next subsection, we quantify the idea of order in terms of the value of A.

The lowest-order solutions are obtained immediately on setting $A = 0$ in equations (8) and (9). These are

$$\Theta = a\cos\theta + b \tag{10}$$

and

$$R = c[r + 2M\ln(r-2M)] + d, \tag{11}$$

where a, b, c and d are constants. The nature of the solutions is

discussed in detail in Section 4. Note that the special case of $c = 0$, the Schwarzschild monopole, was one of the first solutions to be found. Note further that the special case of $a + b = 0$ and $d = 0$ is that of the separable Schwarzschild paraboloid, the non-separable analogue of which has been reported (BZ; M84) and is discussed later. Finally, note the logarithmic singularity at $r = 2M$ in equation (11), which is also discussed later.

3.2 Solutions of general order

We now give a complete characterization of the general solutions of equations (8) and (9), to be labelled by the ordinal number, m, which is defined in terms of the separation constant as

$$A = m(m + 1). \tag{12}$$

With the aid of equation (12), the equation for the angular function Θ becomes

$$(1 - x^2)\frac{\mathrm{d}^2\Theta}{\mathrm{d}x^2} + m(m + 1)\Theta = 0, \tag{13}$$

where $x = \cos\theta$. Similarly, the equation for the radial function R becomes

$$(1 - z^2)\frac{\mathrm{d}^2R}{\mathrm{d}z^2} - 2\frac{\mathrm{d}R}{\mathrm{d}z} + m(m + 1)R = 0, \tag{14}$$

where $z = r/M - 1$.

3.3 The angular function

Solutions of equation (13) are closely related to the Gegenbauer polynomials (see e.g. Szegö 1939, hereafter SZ; Abramowitz & Stegun 1972, hereafter AS; Gradshteyn & Ryzhik 1990, hereafter GR), the angular function of order m being given by

$$\Theta_m(x) = (1 - x^2)\mathcal{C}^{(3/2)}_{m-1}(x), \tag{15}$$

where $\mathcal{C}^{(3/2)}_{m-1}$ are Gegenbauer polynomials. Explicit forms for $\mathcal{C}^{(3/2)}_{m-1}$ can be obtained with the aid of recursion relations, starting with expressions for $\mathcal{C}^{(3/2)}_0$ and $\mathcal{C}^{(3/2)}_1$ (SZ). We list the first few below. Note that we shall hereafter suppress the superscript in $\mathcal{C}^{(3/2)}_{m-1}$ because the values remain the same throughout this work.

$$m = 1, \quad \mathcal{C}_0(x) = 1,$$

$$m = 2, \quad \mathcal{C}_1(z) = 3x,$$

$$m = 3, \quad \mathcal{C}_2(z) = \frac{15}{2}x^2 - \frac{3}{2}. \tag{16}$$

The detailed angular structure of the solutions is discussed in Section 4. Note that the $m = 1$ solution has dipolar symmetry $\Theta_1 \sim \sin^2\theta$, the $m = 2$ solution has quadrupolar symmetry $\Theta_2 \sim \sin^2\theta\cos\theta$, and so on. This is in keeping with our experience of flat-space electrodynamics.

3.4 The radial function

Solutions of equation (14), which are closely related to the Jacobi polynomials and Jacobi functions of the second kind (see SZ for an excellent review), are given by (AS, GR, SZ)

$$R_m(z) \sim (1 + z)^2\begin{cases}\mathcal{P}^{(0,2)}_{m-1}(z)\\ \mathcal{Q}^{(0,2)}_{m-1}(z)\end{cases}, \tag{17}$$

where $\mathcal{P}^{(0,2)}_{m-1}$ are Jacobi polynomials and $\mathcal{Q}^{(0,2)}_{m-1}$ are Jacobi functions of the second kind. The radial function of order m is therefore given by

$$R_m(r) = r^2\begin{cases}\mathcal{P}^{(0,2)}_{m-1}[(r/M) - 1]\\ \mathcal{Q}^{(0,2)}_{m-1}[(r/M) - 1]\end{cases}. \tag{18}$$

The Jacobi polynomials and the Jacobi functions of the second kind represent two distinct classes of radial solutions, of which the physical natures are evident from the asymptotic behaviour displayed at large values of r. For $r \gg M$, the Jacobi polynomial and Jacobi function scalings are (AS, SZ)

$$\mathcal{P}^{(0,2)}_{m-1} \sim r^{m-1}, \quad \mathcal{Q}^{(0,2)}_{m-1} \sim r^{-m-2}, \tag{19}$$

so that the radial function scales as

$$R_m(r) = \begin{cases} r^{m+1}\\ r^{-m}\end{cases} \tag{20}$$

in the two cases, which is immediately reminiscent of the behaviour of the 'interior' and 'exterior' solutions of flat-space electrodynamics. Indeed, as $r \gg M$ is the flat-space limit of the Schwarzschild results, the analogy is quite exact. Therefore, we henceforth refer to the solutions bearing the Jacobi polynomials as the interior solutions, and those bearing the Jacobi functions of the second kind as the exterior solutions. Since the two types of solutions have different mathematical properties and physical significance, we treat them separately.

3.4.1 Interior solutions

Explicit forms for Jacobi polynomials can be obtained from the references listed previously: here we list the first few. Note that henceforth we suppress the two superscripts in $\mathcal{P}^{(0,2)}_{m-1}$, as we use the same values throughout in this work.

$$m = 1, \quad \mathcal{P}_0(z) = 1,$$

$$m = 2, \quad \mathcal{P}_1(z) = 2z - 1,$$

$$m = 3, \quad \mathcal{P}_2(z) = \frac{15}{4}z^2 - \frac{5}{2}z - \frac{1}{4}. \tag{21}$$

For our purposes, it is useful to scale the radial function $R_m(r)$ in terms of the asymptotic value of the function given in equation (20). We combine equations (17) and (21), and obtain

$$R_m(r) = r^{m+1}\mathcal{G}_m(M/r) \tag{22}$$

where $\mathcal{G}_m(M/r)$ is a polynomial that describes the general-relativistic effects. The first few of these polynomials are

$$m = 1, \quad \mathcal{G}_1(x) = 1,$$

$$m = 2, \quad \mathcal{G}_2(x) = 1 - \frac{3}{2}x,$$

$$m = 3, \quad \mathcal{G}_3(x) = 1 - \frac{8}{3}x + \frac{8}{5}x^2. \tag{23}$$

The structure of the interior solutions is discussed in Section 4.

3.4.2 Exterior solutions

As the explicit forms of Jacobi functions of the second kind are not easily found in the standard references, we describe them here at the level of detail adequate for our purposes. We introduce a

prescription for obtaining a general function of this type, $\mathcal{Q}_n^{(\alpha,\beta)}$, which, to our knowledge, is not found in the standard mathematical references. We suggest that explicit forms for $\mathcal{Q}_n^{(\alpha,\beta)}$ can be found most conveniently by the following prescription, through the use of recursion relations, starting with a suitable (integral or differential) representation for $\mathcal{Q}_0^{(\alpha,\beta)}$.

For arbitrary values of α and β satisfying the constraint $\alpha + \beta + 1 > 0$, a useful integral representation (SZ) for $\mathcal{Q}_0^{(\alpha,\beta)}$ is

$$\mathcal{Q}_0^{(\alpha,\beta)}(z) = -2^{\alpha+\beta}\frac{\Gamma(\alpha+1)\Gamma(\beta+1)}{\Gamma(\alpha+\beta+1)}\int_\infty^z \frac{\mathrm{d}t}{(t-1)^{\alpha+1}(t+1)^{\beta+1}}. \tag{24}$$

For positive integral values of α and β, as in our case, a differential representation, which leads to much faster calculation of explicit expressions for $\mathcal{Q}_0^{(\alpha,\beta)}$, can be obtained from equation (24). The representation is

$$\mathcal{Q}_0^{(\alpha,\beta)}(z) = \frac{(-1)^{\beta+1}2^{\alpha+\beta}}{\Gamma(\alpha+\beta+1)} \times \left\{\frac{\mathrm{d}^\alpha}{\mathrm{d}a^\alpha}\frac{\mathrm{d}^\beta}{\mathrm{d}b^\beta}\left[\frac{1}{a+b}\ln\left(\frac{z-a}{z+b}\right)\right]\right\}_{a=b=1}, \tag{25}$$

and we have *not* found it in any standard reference. To prove equation (25), consider the identity

$$\int_\infty^z \frac{\mathrm{d}t}{(t-a)(t+b)} = \frac{1}{a+b}\ln\left(\frac{z-a}{z+b}\right). \tag{26}$$

Differentiation of both sides of equation (26) α times with respect to a and β times with respect to b, and comparison with equation (24), leads to equation (25).

Recursion relations from which $\mathcal{Q}_n^{(\alpha,\beta)}$ with $n > 0$ can be obtained are as follows (SZ). The relation used for calculating $\mathcal{Q}_1^{(\alpha,\beta)}$ is a special one:

$$\mathcal{Q}_1^{(\alpha,\beta)}(z) = \frac{1}{2}[(\alpha+\beta+2)z + \alpha - \beta] \times \mathcal{Q}_0^{(\alpha,\beta)}(z) - 2^{\alpha+\beta-1}\frac{\alpha+\beta+2}{(z-1)^\alpha(z+1)^\beta} \times \frac{\Gamma(\alpha+1)\Gamma(\beta+1)}{\Gamma(\alpha+\beta+2)}. \tag{27}$$

For $n \geqslant 2$, $\mathcal{Q}_n^{(\alpha,\beta)}$ are obtained by repeated application of the general relation that holds for $n \geqslant 2$, namely

$$\begin{aligned} &2n(n+\alpha+\beta)(2n+\alpha+\beta-2)\mathcal{Q}_n^{(\alpha,\beta)}(z) \\ &= (2n+\alpha+\beta-1)[(2n+\alpha+\beta)(2n+\alpha+\beta-2)z \\ &\quad + \alpha^2 - \beta^2]\mathcal{Q}_{n-1}^{(\alpha,\beta)}(z) - 2(n+\alpha-1)(n+\beta-1) \\ &\quad \times (2n+\alpha+\beta)\mathcal{Q}_{n-2}^{(\alpha,\beta)}(z). \end{aligned} \tag{28}$$

We now set $\alpha = 0$ and $\beta = 2$ for our problem, and calculate Jacobi functions of interest from equations (25), (27) and (28). We present the first few below, and henceforth suppress the two superscripts in $\mathcal{Q}_{m-1}^{(0,2)}$, since the values of the superscripts remain the same throughout this work:

$$m = 1, \quad \mathcal{Q}_0(z) = \frac{1}{2}\ln\left(\frac{z+1}{z-1}\right) - \frac{z+2}{(z+1)^2},$$

$$m = 2, \quad \mathcal{Q}_1(z) = \left(z - \frac{1}{2}\right)\ln\left(\frac{z+1}{z-1}\right) - \frac{2z^2+3z+2/3}{(z+1)^2},$$

$$m = 3, \quad \mathcal{Q}_2(z) = \left(\frac{15}{8}z^2 - \frac{5}{4}z - \frac{1}{8}\right)\ln\left(\frac{z+1}{z-1}\right) - \frac{(15/4)z^3 + 5z^2 - z/4 - 4/3}{(z+1)^2}. \tag{29}$$

The structure of the exterior solutions is discussed in Section 4. Note the appearance of a logarithmic singularity in the term $\ln(r - 2M)$ at $\mathcal{H}$ in these solutions (z in equation 29 is defined as $z = r/M - 1$, see above); the singularity also appeared in one of the lowest-order solutions discussed above. This singularity is reminiscent of the one that occurs in the well-known flat-space exterior solutions (in the term r^{-m}) at $r = 0$, but it is weaker. Of course the appearance of such a singularity does not imply that the exterior solutions for black hole electrodynamics are invalid, any more than does the appearance of the power-law singularity in the flat-space exterior solutions: it simply means that these exterior solutions are valid in the regions of space that exclude $\mathcal{H}$, just as the regions of validity of the flat-space exterior solutions necessarily exclude the origin. We will return to this point in Sections 4 and 5. Finally, we note that the power-law singularity, displayed by the Jacobi functions of equation (29) at $r = 0$ (i.e. $z + 1 = 0$), has no physical significance since these solutions do not apply for $r < 2M$.

4 STRUCTURE OF THE SOLUTIONS

4.1 Lowest-order solutions

The solution corresponding to $c = 0$ in equation (11), i.e.

$$\psi \sim a\cos\theta + b, \tag{30}$$

where a and b are constants, is the Schwarzschild monopole, the field lines of which are shown in Fig. 1.

This solution has been discussed previously by BZ and M84, and the flat-space version (identical in form to equation 30) has been discussed by M73. We impose the solenoidal condition upon $\boldsymbol{B}$, which must be satisfied in all astrophysical applications, by using the device of assigning opposite polarities to the radial magnetic field in the two hemispheres (BZ; M84). This is the so-called 'split monopole' configuration maintained by a toroidal current in the accretion disc lying in the equatorial plane. The results of spinning up the split monopole field have been described in various approximations by BZ and M84, and the exact solution of the flat-space analogue was given by M73.

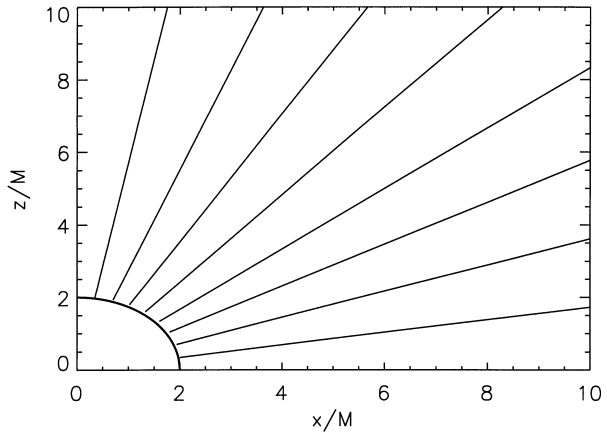

Figure 1. Poloidal field lines of the Schwarzschild monopole. The horizon $\mathcal{H}$ is shown by the thick line. All lengths are in natural units, as indicated.

The solution corresponding to $a + b = 0$ and $d = 0$, i.e.

$$\psi \sim [r + 2\ln(r - 2M)](1 - \cos\theta), \tag{31}$$

represents the separable Schwarzschild paraboloid [our nomenclature comes from the observation that in equation (31) the sole difference between this paraboloid and the familiar flat-space paraboloid is the presence of a logarithmic term characteristic of Schwarzschild space–time]. The field lines of the paraboloid are shown in Fig. 2.

At sufficiently large radii, this configuration reduces to the paraboloidal field lines of flat-space electrodynamics, which have been studied at length by B76. For small radii, the separable Schwarzschild paraboloid has one curious relativistic feature: close to $\mathcal{H}$ the field lines change direction so that ψ, which is a measure of the magnetic flux (see Section 2), changes sign. For the specific stream function given in equation (31), ψ changes sign at $r \approx 2.314M$. Note that this asymptotically paraboloidal separable solution is similar to the corresponding non-separable solution (BZ; M84), which we discuss in Section 5, but there are also clear differences between the two.

4.2 General solutions

We now combine the angular and radial parts of the general solutions for the stream function described in Section 3, and discuss the structure of the resultant field configurations.

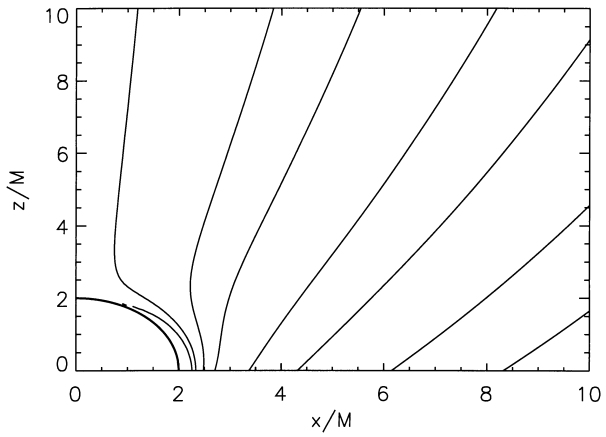

Figure 2. Same as Fig. 1, but for the separable Schwarzschild paraboloid.

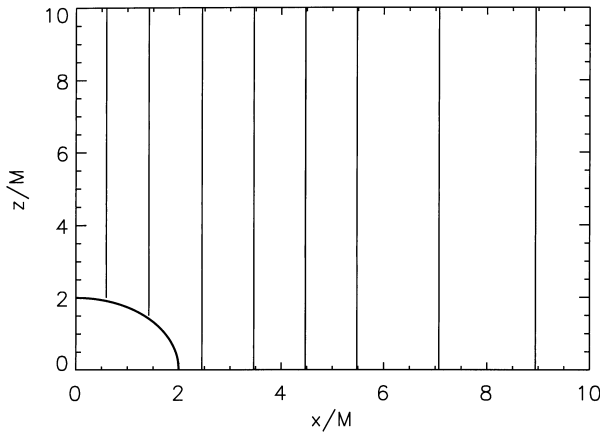

Figure 3. Same as Fig. 1, but for the uniform field in Schwarzschild space–time.

4.2.1 *Interior solutions*

The stream function for $m = 1$, namely

$$\psi_1 \sim r^2 \sin^2\theta, \tag{32}$$

represents a uniform magnetic field pointing in the z-direction, as shown in Fig. 3.

As a result of the apparent simplicity of this configuration, this appears to be the most thoroughly studied (Wald 1974; Hanni & Ruffini 1976; M84) field configuration in Schwarzschild space–time. The configuration is identical to that obtained in flat-space electrodynamics corresponding to the $m = 1$ term of a multipolar decomposition of the scalar potential, i.e. $\Phi_1 = rP_1(\cos\theta)$ (here P_1 is a Legendre polynomial).

The stream function for $m = 2$, namely

$$\psi_2 \sim \left(r^3 - \frac{3}{2}Mr^2\right)\sin^2\theta\cos\theta, \tag{33}$$

represents the interior solution of the next higher order, the field lines of which are shown in Fig. 4.

This configuration is very similar, but not identical, to that obtained in flat-space electrodynamics corresponding to the $m = 2$ term of a multipolar decomposition of the scalar potential, i.e. $\Phi_2 = r^2P_2(\cos\theta)$.

The structure of higher-order solutions may be readily obtained in a similar manner. It is this term-by-term analogy with well-known configurations in flat-space electrodynamics that makes our scheme of classifying the field configurations in curved space–time particularly transparent, and underscores the power of the 3 + 1 formalism.

4.2.2 *Exterior solutions*

The stream function for $m = 1$, namely

$$\psi_1 \sim \left[\frac{r^2}{2}\ln\left(\frac{r}{r - 2M}\right) - rM - M^2\right]\sin^2\theta, \tag{34}$$

represents a solution which we name the Schwarzschild dipole. The field lines, shown in Fig. 5, readily explain the terminology

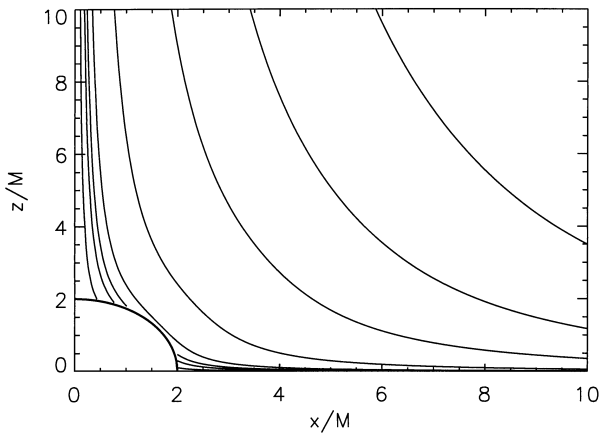

Figure 4. Same as Fig. 1, but for the $m = 2$ interior solution.

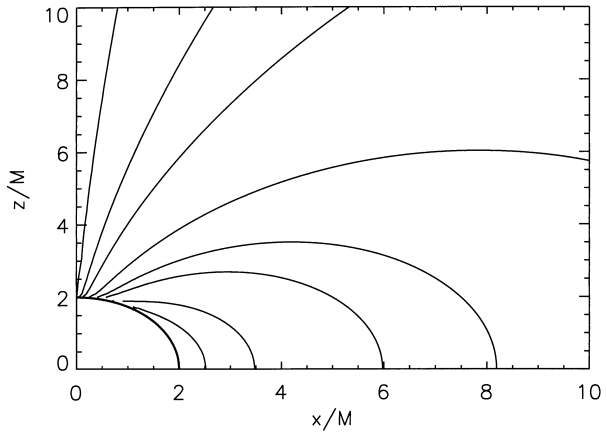

Figure 5. Same as Fig. 1, but for the Schwarzschild dipole.

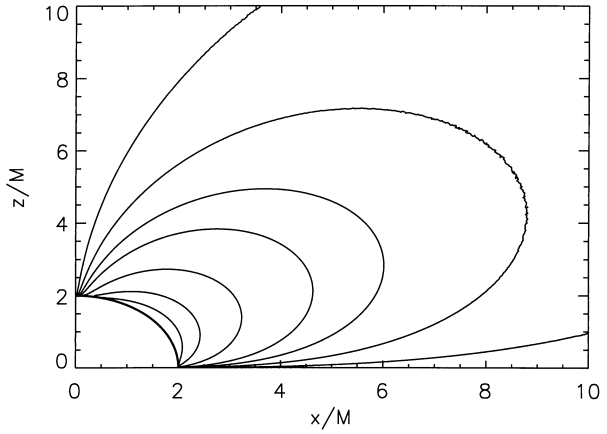

Figure 6. Same as Fig. 1, but for Schwarzschild quadrupole.

by demonstrating that this solution is the Schwarzschild analogue of the familiar flat-space dipole field.

The analogy is quite exact as, on taking the limit $r \gg M$ in equation (34), we find that $\psi_1 \sim (1/r)\sin^2\theta$, which describes the field lines of a flat-space dipole.

Similarly, the stream function for $m = 2$, namely

$$\psi_2 \sim \left[\left(r^3 - \frac{3}{2}Mr^2\right)\ln\left(\frac{r}{r-2M}\right) - 2r^2M + rM^2 + \frac{M^3}{3}\right] \times \sin^2\theta\cos\theta, \quad (35)$$

represents the Schwarzschild quadrupole, the field lines of which are displayed in Fig. 6.

The quadrupolar symmetry is evident. The reader can verify the exactness of the flat-space analogy by extracting the $r \gg M$ limit of equation (35) and noting that, in this limit, $\psi_2 =$ constant is precisely the equation for the field lines of a flat-space quadrupole.

The higher exterior multipoles (octupole and so on) may be readily obtained in a similar manner. For the exterior solutions, the exactness of the analogy with the multipoles of flat-space electrodynamics makes the classification scheme completely natural and transparent, and re-emphasizes the virtue of the 3 + 1 formalism.

5 DISCUSSION

5.1 Astrophysical context

The classes of solutions detailed in Sections 3 and 4 provide natural generic choices for appropriate classes of black hole electrodynamics problems involving accretion discs. For studies concerned with field structure, the transport of energy or angular momentum close to the horizon of the hole, our lowest-order and interior solutions (BZ; M84; B97a,b; KMSK) are clearly the best choice (also see Section 5.4). The uniform field configuration corresponding to $m = 1$ describes the essential astrophysics very close to $\mathcal{H}$, as has been intuitively realized long ago (see TPM, particularly their fig. 36). This is a result of the physical mechanisms described in MT and TPM, by which the black hole 'cleans' the magnetic field threading its horizon of details, kinks and closed loops (also see Section 5.3). At slightly larger distances from $\mathcal{H}$ ($\sim\mathcal{R}_\mathcal{H}$, say, where $\mathcal{R}_\mathcal{H}$ is the characteristic scale size of $\mathcal{H}$) further details of field structure begin to appear, even under the most ideal circumstances, owing to the contribution of the currents circulating at the inner edge of the accretion disc. These are described by interior solutions of higher order, $m = 2, 3, \ldots$, of which the relative contributions determine the shape of the beam or jet of relativistic particles transporting energy to the radio lobes. Similar arguments apparently also hold for MHD jets in AGN and quasars, although the stream equation and the structure of the interior solutions are somewhat different in those cases (B97 and references therein).

On the other hand, for describing the field structure on and around the accretion disc at larger distances ($\gg\mathcal{R}_\mathcal{H}$) from $\mathcal{H}$, our exterior solutions are the natural choice. They describe, term by term, the multipole moments of the currents circulating in the disc, as seen by an external observer approaching the hole. The $m = 1$ dipole is thus a first estimate of the total effect of the disc currents, as seen by a distant observer. This decomposition proves particularly useful for analysing the relative effects of currents circulating in the disc and on the horizon of the hole. Astrophysical applications of these field structures to disc-driven jets and MHD winds, and to dynamo-action in discs are well-known (Konigl & Kartje 1994; Khanna & Camenzind 1992, 1996; Camenzind 1995).

Construction of model global field structures relevant to almost all black hole accretion disc problems involves the matching of interior and exterior solutions at a suitable intermediate radius according to a prescription appropriate for the particular problem. This has direct relevance to the 'impedance matching' considerations long known to be crucial to studies of BZ processes and related particle acceleration issues (Lovelace, MacAuslan & Burns 1979; MT; TPM). In fact techniques borrowed from matching procedures in flat-space electrodynamics may provide the most rigorous formulation for impedance matching between the black hole source and the distant astrophysical load (we shall describe this elsewhere).

5.2 Non-separable solutions

Separable solutions do not exhaust all the possibilities for solutions of equation (5). One particular non-separable solution of astrophysical interest is that found by BZ and discussed by M84. It is given by

$$\psi \sim [(r-2M)(1-\cos\theta) - 2M(1+\cos\theta)\ln(1+\cos\theta)], \quad (36)$$

and the corresponding field lines are asymptotically paraboloidal. This solution was used in the original BZ study of the extraction of rotational energy from black holes. Equation (37) is one of the lowest-order, non-separable solutions of equation (5), analogous to the lowest-order separable paraboloid solution described by equation (31). At large radii, both of these solutions reduce to the familiar exact paraboloids of flat-space electrodynamics $\psi_{nr} \sim r(1 - \cos\theta)$; the astrophysical applications of these paraboloids to accretion disc electrodynamics and jet formation have been discussed at length by B76.

However, there is nothing fundamental about the paraboloidal shape in the astrophysical context, except that field lines do need to be asymptotically vertical if electromagnetic energy is to be beamed along the rotation axis of the black hole, as in the BZ process. In fact the asymptotically paraboloidal shapes discussed above have the disadvantage that they have an inflexible shape on the equatorial plane (the ratio B_ϖ/B_z is always unity on this plane in the Newtonian limit), so that it is sometimes impossible to satisfy boundary conditions of astrophysical interest on the accretion disc surface. A good example is discussed in GA where recent numerical simulations of dynamo-generated magnetic fields in accretion discs suggest $B_\varpi/B_z \sim 2$–3 (GA and references therein), which paraboloidal field lines cannot mimic. To achieve this, GA found a solution

$$\psi \sim [(r - 2M)(1 - \cos\theta) - r_0 \cos\theta - 2M(1 + \cos\theta)\ln(1 + \cos\theta)], \quad (37)$$

which was adequate for this kind of modelling. It is clear that the solution given by equation (37) is a linear superposition of those given by equations (36) and (30), and therefore must necessarily be a solution of the linear equation (5). Equations (36) and (37) appear to be the only astrophysically interesting non-separable solutions of equation (5) known at this time.

There is no difficulty in obtaining further non-separable solutions by superposing equation (36) with other classes of separable solutions found in this work, but this is not of basic importance. A systematic method of classifying higher-order non-separable solutions would be more important both in principle and in the astrophysical context (this will be discussed elsewhere).

5.3 The MT theorem

MT proved an interesting theorem (hereafter referred to as the MT theorem), which states that closed loops of magnetic field threading $\mathcal{H}$ cannot exist in stationary axisymmetric force-free magnetospheres. Therefore, a natural question which may arise at this point is: how do the external solutions found here, all of which have closed loops extending to $\mathcal{H}$, stand *vis-à-vis* the MT theorem?

To answer this question, consider first the proof of the MT theorem. As we are concerned here only with Schwarzschild black holes, we shall be content with the proof for this case, which is particularly simple. Since equation (5) implies that the vector $(\aleph/\varpi^2)\nabla\psi$ is solenoidal, we can convert it, by Gauss's theorem, into the condition that the surface integral of the vector, over a closed surface $\mathcal{L}$ that consists of a closed loop and the region between its footpoints on $\mathcal{H}$, vanishes:

$$\int_{\mathcal{L}} \frac{\aleph}{\varpi^2} \nabla\psi \, \mathrm{d}\boldsymbol{S} = 0. \quad (38)$$

Here, $\mathrm{d}\boldsymbol{S}$ is an element of surface area along the outward direction of the normal. Now, MT considered stream functions (and the related derivatives) that remained finite on $\mathcal{H}$. Their argument then suggested that as the lapse function $\aleph$ (by definition) vanishes on $\mathcal{H}$ (see e.g. Bardeen 1973), so does that part of the integral which comes from $\mathcal{H}$, implying that the integral over the closed field loop itself vanishes. However, because the field lines are contours of constant ψ (see Section 2.2), $\nabla\psi$ is parallel to $\mathrm{d}\boldsymbol{S}$ everywhere, so that the integrand has the same sign all over the closed loop. It follows, therefore, that the integral can vanish only if the integrand vanishes everywhere, which means that there can be no field or field loop.

Now consider the results of applying the MT theorem to our closed-loop external solutions. Since the stream functions ψ for these solutions diverge like $\ln\aleph$ on approaching $\mathcal{H}$, as explained earlier (see Section 3.4.2 and equation 4), $\nabla\psi$ diverges as $\aleph^{-1}$. Thus the integrand $(\aleph/\varpi^2)\nabla\psi$ is finite over $\mathcal{H}$, as is the contribution to the integral in equation (38). Depending on the details of the field geometry in the close neighbourhood of $\mathcal{H}$, it may therefore be possible to satisfy equation (38) without requiring that the field be zero everywhere on the closed loop. Thus, the MT theorem is not in contradiction with closed-loop solutions that diverge on $\mathcal{H}$. The situation is closely analogous to that for exterior solutions in flat-space electrodynamics: these solutions, which have closed field loops, diverge at the origin ($r = 0$), and integrals similar to that in equation (38) (or related integrals involving the scalar potential) have to be evaluated carefully in the neighbourhood of the origin, and can include finite contributions from there.

The above discussion does not, of course, imply that the exterior solutions found here can extend up to $\mathcal{H}$. This is ruled out simply because they diverge on $\mathcal{H}$ and are, therefore, physically inadmissible there. As we have previously indicated, the domain in which the exterior solutions remain valid is a region of space that excludes $\mathcal{H}$ (implicit in the use of 'exterior'). Examples of this abound in flat-space electrodynamics, and it is not difficult to envisage model problems in black hole electrodynamics where an inner region containing $\mathcal{H}$ requires interior solutions, surrounded by an outer region that requires exterior solutions: we have already indicated that matching these solutions may be of considerable astrophysical importance.

Finally, the MT theorem only excludes the existence of closed-loop field configurations that remain finite on $\mathcal{H}$. We have shown that all separable Schwarzschild solutions with closed loops diverge on $\mathcal{H}$. The two non-separable solutions known so far do not have closed loops, and consequently it is correct to say that all known Schwarzschild solutions with closed loops diverge on $\mathcal{H}$. This is therefore a *confirmation* of the MT theorem, showing that the configurations shown by MT to be untenable are, indeed, not found among the known solutions. Again, we find a close analogy with multipolar expansion in flat-space electrodynamics, where all of the closed-loop multipole solutions (dipole, quadrupole, etc) diverge at the origin.

5.4 Concluding remarks

Our confidence in the relevance of the poloidal Schwarzschild solutions, found in this work, to electrodynamics around rotating black holes stems largely from the insignificant influence of rotation, except at the highest possible rates, on poloidal field structures found in all cases investigated so far (M84; K98; K99; KMSK; also see below). A remaining concern is the role of the

toroidal field, the strength of which is expected to depend significantly on the rotation rate of the hole (MT). While poloidal and toroidal fields are effectively decoupled, as we argued in Section 2, in most problems of interest in black hole electrodynamics, so that the higher toroidal fields generated by increasing rotation rates do not react back on the poloidal fields, their influences on the essential astrophysical phenomena (e.g. the BZ process) need to be clarified. The key point here is the effect of the well-known boundary conditions on $\mathcal{H}$ (MT and references therein). As we approach $\mathcal{H}$, the poloidal field becomes entirely normal ($\boldsymbol{B}_\perp$) to $\mathcal{H}$, while the toroidal field $\boldsymbol{B}_\mathrm{T}$ diverges as $\aleph^{-1}$, so that $\boldsymbol{B}_\mathrm{H} \equiv \aleph \boldsymbol{B}_\mathrm{T}$ remains finite. The strength of the BZ process scales with the magnetic stress $\boldsymbol{B}_\perp \boldsymbol{B}_H$, but the 'degeneracy' condition ($\boldsymbol{E} \cdot \boldsymbol{B} = 0$) outside $\mathcal{H}$ fixes the ratio $\boldsymbol{B}_\perp / B_H$ in terms of the rotation rate of the hole (GA and references therein), so that the BZ power output finally scales with $\boldsymbol{B}_\perp^2$ alone. Thus, any direct influence of the magnitude of the toroidal field on the strength of this particular astrophysical process ultimately drops out, and a sufficiently accurate estimate of the poloidal field close to $\mathcal{H}$ is all that one needs to calculate the strength of the BZ process and related quantities, for a black hole with a specified rotation rate. This is why our poloidal field calculations are expected to be of considerable practical value in BZ-process calculations relevant to double radio sources, AGN and quasars, and also to the poloidal field structures associated with relativistic jets in AGN and microquasars. However, there are other astrophysical phenomena that do depend crucially on the strength of $\boldsymbol{B}_\mathrm{T}$ away from the horizon, such as the collimation and stability of the above jets (Appl & Camenzind 1992; K99; KMSK). We expect, therefore, that adequate investigations of these phenomena will require reliable calculations of the toroidal field structure of the magnetospheres of rotating black holes, which is beyond the scope of this work.

After the original version of this paper was submitted, we became aware of an excellent contemporaneous review (B97) on axisymmetric stationary flows in astrophysical objects, in which a model black hole magnetosphere is constructed by expanding the non-relativistic M73 solution, and introducing relativistic effects into each term separately. The final result, given in two terms, seems to be similar to a combination of our interior solutions with $m = 1,\ 3$; the $m = 2$ term vanishes for the particular solution considered by B97 because of symmetry properties. We also note the similarity between the poloidal structure of our separable Schwarzschild paraboloid (Fig. 2), and that of the numerical computation in F97 of collimated jet magnetospheres in Kerr space–time (fig. 3 of F97): this may well be indicative of the secondary importance of the rotation of the hole to the magnetospheric structure that we have suggested in this paper. Finally, the results of recent simulations of jet formation by Koide and collaborators (K98; K99; KMSK), with the aid of their general relativistic MHD code, clearly support our conclusions. The poloidal field structures around rapidly rotating Kerr holes (KMSK) are found by these authors to be very similar to those around Schwarzschild holes (K98), particularly for co-rotating Keplerian discs, confirming a major argument used in this paper. Further, these authors begin their simulations with a uniform poloidal magnetic field (our interior solution with $m = 1$, as shown in our Fig. 3), and obtain poloidal structures at the end of the simulations that appear remarkably similar to our separable Schwarzschild paraboloid (a lowest-order solution shown in our Fig. 2), for both Schwarzschild holes (fig. 2 of K98) and rapidly rotating Kerr holes (fig. 1d of KMSK) accreting from co-rotating Keplerian discs. This gives us great confidence in the relevance of the basic 'building block' poloidal field structures found in this work to essential astrophysical processes near black holes: future simulations should fully exploit our multipolar expansion scheme.

REFERENCES

Abramowitz M., Stegun I. A., 1972, Handbook of Mathematical Functions. Dover Publications, New York (AS)
Appl S., Camenzind M., 1992, A&A, 256, 354
Appl S., Camenzind M., 1993, A&A, 274, 699
Balbus S. A., Hawley J. F., 1998, Rev. Mod. Phys., 70, 1
Bardeen J. M., 1973, in Dewitt C., Dewitt B. S., eds, Black Holes. Gordon & Breach, New York
Bardeen J. M., Press W. H., Teukolsky S. A., 1973, ApJ, 178, 347
Beskin V. S., 1997, Usp. Fiz. Nauk, 167, 689 (B97)
Beskin V. S., 1997, Usp. Fiz. Nauk, 167, 689 (B97) (Sov. Phys. – Usp., 40, 659, English translation)
Blandford R. D., 1976, MNRAS, 176, 465 (B76)
Blandford R. D., 1998, in Holt S. S., Kallman T. R., eds, Accretion Processes In Astrophysical Systems: Some Like It Hot. Am. Inst. Phys., New York, p. 43
Blandford R. D., Znajek R. L., 1977, MNRAS, 179, 433 (BZ)
Brandenburg A., Nordlund A., Stein R. F., Torkelsson U., 1995, ApJ, 446, 741
Camenzind M., 1995, Rev. Mod. Astron., 8, 201
Eikenberry S. S., Matthews K., Morgan E. H., Remillard R. A., Nelson R. W., 1998, ApJ, 494, L61
Fendt C., 1997, A&A, 319, 1025 (F97)
Ghosh P., Abramowicz M. A., 1997, MNRAS, 292, 887 (GA)
Gradshteyn I. S., Ryzhik I. M., 1990, Table of Integrals, Series, and Products. Academic Press, New York (GS)
Hanni R. S., Ruffini R., 1976, Nuovo Cimento Lett., 15, 189
Khanna R., Camenzind M., 1992, A&A, 263, 401
Khanna R., Camenzind M., 1996, A&A, 307, 665
Koide S., Shibata K., Kudoh T., 1998, ApJ, 495, L63 (K98)
Koide S., Shibata K., Kudoh T., 1999, ApJ, 522, 727 (K99)
Koide S., Meier D. L., Shibata K., Kudoh T., 2000, ApJ, submitted (astro-ph/9907435) (KMSK)
Königl A., Kartje J. F., 1994, ApJ, 434, 446
Lovelace R. V. E., MacAuslan J., Burns M., 1979, in Arons J., McKee C., Max C., eds, AIP Conf. Proc. 56, Particle Acceleration Mechanisms in Astrophysics. Am. Inst. Phys., New York, p. 399
Macdonald D., 1984, MNRAS, 211, 313 (M84)
Macdonald D., Thorne K. S., 1982, MNRAS, 198, 345 (MT)
Michel F. C., 1973, ApJ, 180, 207 (M73)
Szegö G., 1939, Orthogonal Polynomials. Am. Math. Soc., New York (SZ)
Thorne K. S., Macdonald D., 1982, MNRAS, 198, 339 (TM)
Thorne K. S., Price R. H., Macdonald D., 1986, Black Holes: The Membrane Paradigm. Yale Univ. Press, New Haven, p. 132–145 (TPM)
Wald R. M., 1974, Phys. Rev. D, 10, 1680

This paper has been typeset from a TEX/LATEX file prepared by the author.